IMMUNOBIOLOGY AND IMMUNOTHERAPY

c-MPL provides tumor-targeted T-cell receptor-transgenic T cells with costimulation and cytokine signals

Christopher D. Nishimura,[1] Daniel A. Brenner,[1,2] Malini Mukherjee,[1,2] Rachel A. Hirsch,[3] Leah Ott,[1] Meng-Fen Wu,[4] Hao Liu,[4] Olga Dakhova,[1] Jordan S. Orange,[2,5] Malcolm K. Brenner,[1,3,5,6] Charles Y. Lin,[3] and Caroline Arber[1,6]

[1]Center for Cell and Gene Therapy, Baylor College of Medicine, Houston Methodist Hospital and Texas Children's Hospital, Houston, TX; and [2]Center for Human Immunobiology, [3]Department of Molecular and Human Genetics, [4]Department of Biostatistics, Dan L. Duncan Comprehensive Cancer Center, [5]Department of Pediatrics, and [6]Department of Medicine, Baylor College of Medicine, Houston, TX

Key Points

- c-MPL enables tumor-directed TCR$^+$ T cells to become sequential killers by improving immune synapses, costimulation, and cytokine signals.
- c-MPL activation improves in vivo persistence and antitumor function of adoptively transferred c-MPL$^+$ TCR-transgenic T cells.

Adoptively transferred T-cell receptor (TCR)-engineered T cells depend on host-derived costimulation and cytokine signals for their full and sustained activation. However, in patients with cancer, both signals are frequently impaired. Hence, we developed a novel strategy that combines both essential signals in 1 transgene by expressing the nonlymphoid hematopoietic growth factor receptor c-MPL (myeloproliferative leukemia), the receptor for thrombopoietin (TPO), in T cells. c-MPL signaling activates pathways shared with conventional costimulatory and cytokine receptor signaling. Thus, we hypothesized that host-derived TPO, present in the tumor microenvironment, or pharmacological c-MPL agonists approved by the US Food and Drug Administration could deliver both signals to c-MPL-engineered TCR-transgenic T cells. We found that c-MPL$^+$ polyclonal T cells expand and proliferate in response to TPO, and persist longer after adoptive transfer in immunodeficient human TPO-transgenic mice. In TCR-transgenic T cells, c-MPL activation enhances antitumor function, T-cell expansion, and cytokine production and preserves a central memory phenotype. c-MPL signaling also enables sequential tumor cell killing, enhances the formation of effective immune synapses, and improves antileukemic activity in vivo in a leukemia xenograft model. We identify the type 1 interferon pathway as a molecular mechanism by which c-MPL mediates immune stimulation in T cells. In conclusion, we present a novel immunotherapeutic strategy using c-MPL-enhanced transgenic T cells responding to either endogenously produced TPO (a microenvironment factor in hematologic malignancies) or c-MPL-targeted pharmacological agents. (Blood. 2017;130(25):2739-2749)

Introduction

T cells modified with a transgenic T-cell receptor (TCR) can efficiently target intracellular tumor-associated antigens processed and presented on the cell surface in the context of major histocompatibility complex molecules.[1,2] These tumor-associated antigens include lineage differentiation antigens, cancer testis antigens, and the inhibitor of apoptosis protein, survivin.[3] Although transgenic TCRs mediate specific target antigen recognition (signal 1), TCR-transgenic T cells lack built-in transgenic costimulation (signal 2) to enhance antigen-specific responses, a distinction from second-generation chimeric antigen receptor-modified T cells.[2,4] Most engineered T cells of both types rely on host-derived cytokine signals (signal 3) for their sustained in vivo function and persistence, but levels vary in individual patients. In addition, cytokines may not efficiently reach the tumor site where they are most needed for the support of adoptively transferred T cells. A cytokine milieu more favorable to expansion and effector function can be induced by administration of lymphodepleting chemotherapy to the patient before adoptive T-cell therapy, but may be insufficiently sustained for optimal antitumor activity. We therefore investigated whether a single additional gene modification incorporating both

signals 2 and 3 would more consistently and controllably improve TCR-transgenic T-cell persistence and antitumor function in vivo, with a receptor that responds both to a tumor microenvironment factor and to pharmacological agents.

The hematopoietic growth factor receptor c-MPL (myeloproliferative leukemia) is the receptor for thrombopoietin (TPO) and is expressed in hematopoietic stem cells (HSCs) and progenitor cells of the myelo/megakaryocytic lineage.[5] c-MPL is involved in self-renewal, expansion, and maintenance of the HSC pool and stimulation of megakaryocytic progenitor cells supporting platelet production and maturation, but is not expressed in lymphoid lineage cells.[6-8] TPO is produced in the liver and kidneys and in the bone marrow (BM) microenvironment by stem cell niche cells, where it locally supports HSCs and progenitors[9,10]; its systemic levels are tightly regulated by c-MPL-mediated TPO scavenging,[11] as well as sensing of aged platelets by the Ashwell-Morell receptor in the liver.[12] TPO binding to c-MPL activates several signaling pathways including JAK2/STAT, PI3K/Akt, and Raf-1/MAP kinase, in addition to activation of its negative regulator SOCS-3.[5] Thus, c-MPL-activated pathways significantly

overlap with common pathways used by T-cell costimulatory molecules (eg, CD28),[13] as well as common γ-chain cytokine receptors (eg, IL-2, IL-4, IL-7, IL-9, IL-15, IL-21),[14] so that human T cells engineered to express a transgenic c-MPL receptor should receive both costimulatory (signal 2) and cytokine (signal 3) signals upon c-MPL activation. We therefore determined whether systemic TPO levels in steady state could provide homeostatic expansion signals to c-MPL-transgenic T cells, whether local BM microenvironment TPO levels were sufficient to support local antitumor function and persistence of tumor-associated antigen-specific TCR-transgenic c-MPL$^+$ T cells that targeted hematologic malignancies, and whether pharmacologic support of c-MPL$^+$ TCR-transgenic T cells could further enhance their antitumor activity.

We now show that c-MPL can be efficiently expressed in polyclonal as well as tumor-targeted TCR-transgenic T cells. c-MPL activation of T cells under steady-state conditions increases T-cell persistence and enhances the antitumor activity of TCR-transgenic T cells in vitro and in vivo. In addition to increased T-cell expansion and persistence, c-MPL activation of transgenic T cells increased their cytokine production and led to more efficient immune synapse formation; these effects were associated with significant changes in gene expression signatures affecting pro-inflammatory and cell cycle pathways. Hence, c-MPL can mediate both costimulation and cytokine signals (2 and 3) in T cells, and thereby improve their antitumor activities.

Methods

Cell lines

BV173, U266B1, K562, and 293T cell lines were purchased and maintained as described. The BV173.ffLuc cell line was previously described.[15] The K562 cell line engineered to express HLA-A*0201, CD40L, CD80, and OX40L[16] was used as artificial antigen-presenting cells for T-cell expansion experiments.

Blood samples from healthy donors

Buffy coats were procured from de-identified healthy volunteers at the Gulf Coast Regional Blood Center (Houston, TX).

Generation of retroviral vectors

The c-MPL plasmid was kindly provided by Patrick Barth (Baylor College of Medicine, Houston, TX), and the survivin-specific TCR has been described previously.[15] Retroviral constructs were generated using the In-Fusion HD Cloning Kit (Clontech).

Generation of retroviral supernatant and transduced T cells

Transient retroviral supernatant was prepared by transfection of 293T cells, and activated T cells were transduced as described.[15] The number of retroviral integrants in TCR$^+$c-MPL$^+$ T cells was estimated by quantitative polymerase chain reaction.

Immunophenotyping

Cells were stained with antibodies and reagents indicated in supplemental Methods, available on the *Blood* Web site, and analyzed by flow cytometry.

Sequential coculture assay

BV173 or U266B1 cells and T cells were cocultured in up to 8 replicate wells at various E:T ratios. Every 3 to 4 days, cells were harvested from a replicate culture well and analyzed by fluorescence-activated cell sorter (FACS) for tumor cell and T-cell counts, as well as T-cell memory marker phenotype. Fresh tumor cells, IL-2 (25 U/mL), rhTPO (Peprotech), or eltrombopag (EP; MedKoo), were added

back at the same concentrations to untouched replicate wells. Cocultures on anti-CD28-coated plates (1 μg/mL; BD) were transferred to new plates at each point.

Multiplex cytokine assay

Coculture supernatants were analyzed by the MILLIPLEX human Th17 or human CD8$^+$ T-cell Magnetic Bead Panel (EMD Millipore) and Luminex 200.

Immunological synapse imaging

T cells isolated from sequential killing cocultures and fresh BV173 target cells were mixed at E:T 1:2, incubated for 10 minutes, fixed, permeabilized, stained with antibodies indicated in supplemental Methods, and analyzed on a Leica TCS SP8 laser scanning microscope.

RNA sequencing

Total RNA was extracted and sent to GENEWIZ for library preparation and sequencing, with 30 million reads per sample at a 1×50 base pair configuration. Data analysis is described in supplemental Methods.

Mouse xenograft models

In the first model, T-cell persistence, unirradiated female hTPOtg-RAG2$^{-/-}$ γc$^{-/-}$ mice received 2 IV (retro-orbital) doses of 10^7 GFP-ffLuc$^+$ T cells/mouse. T-cell persistence was followed by in vivo bioluminescent imaging (BLI; Caliper Life Sciences) and FACS analysis of peripheral blood of mice. In the second model, antitumor activity, male or female hTPOtg-RAG2$^{-/-}$ γc$^{-/-}$ mice were irradiated with 200 cGy and injected IV (tail vein) with 3×10^6 BV173.ffluc cells. The following day, 5×10^6 T cells/mouse were injected IV (retro-orbitally).

A detailed description of all methods is available in supplemental Information.

Results

c-MPL expression in polyclonal T cells leads to agonist-dependent T-cell expansion and persistence

To test whether c-MPL can be expressed efficiently in polyclonal T cells, we constructed a retroviral vector encoding the c-MPL gene (supplemental Figure 1A) and transduced activated polyclonal T cells. Transduction efficiencies were high in both CD4$^+$ and CD8$^+$ T cells ($1.6 \pm 0.5\%$ nontransduced [NT] vs $76.3 \pm 10.9\%$ c-MPL transduced [c-MPL$^+$] cells; mean $\pm$ SD; n = 5; $P < .001$; Figure 1A). c-MPL$^+$ T cells expanded (Figure 1B) and proliferated (Figure 1C) in the presence of recombinant human thrombopoietin (TPO) during the first week at a similar rate to cells cultured in IL-2 (P = NS), whereas c-MPL$^-$ control cells did not ($0.89 \pm 0.61 \times 10^6$ NT vs $7.44 \pm 0.99 \times 10^6$ c-MPL$^+$ cells in TPO by day 7 from 3×10^6 cells [mean $\pm$ SD]; n = 4, $P < .001$; Figure 1B). Peak expansion was observed after 1 week of culture, followed by a steady decline in T-cell numbers in the absence of repeated TCR stimulation (supplemental Figure 2). No growth factor-independent cell growth was observed. Activation of c-MPL downstream signaling was assessed by Phosflow for pSTAT5 protein (Figure 1D). STAT5 phosphorylation occurred in c-MPL$^+$ T cells in response to rhTPO at 5 and 50 ng/mL, or with the small molecule TPO mimetic drug EP (0.1 μg/mL). We next evaluated the in vivo persistence of polyclonal c-MPL$^+$ T cells under homeostatic steady-state cytokine conditions in immune-deficient human-TPO transgenic (hTPOtg-RAG2$^{-/-}$γc$^{-/-}$) mice.[17] Unconditioned steady-state hTPOtg-RAG2$^{-/-}$γc$^{-/-}$ mice were infused IV with 10^7 GFP-ffLuc tagged control or c-MPL$^+$ T cells in the retro-orbital venous plexus for 2 consecutive doses, 6 days apart, followed by in vivo BLI (Figure 1E-F). c-MPL$^+$ T cells had increased systemic persistence compared with
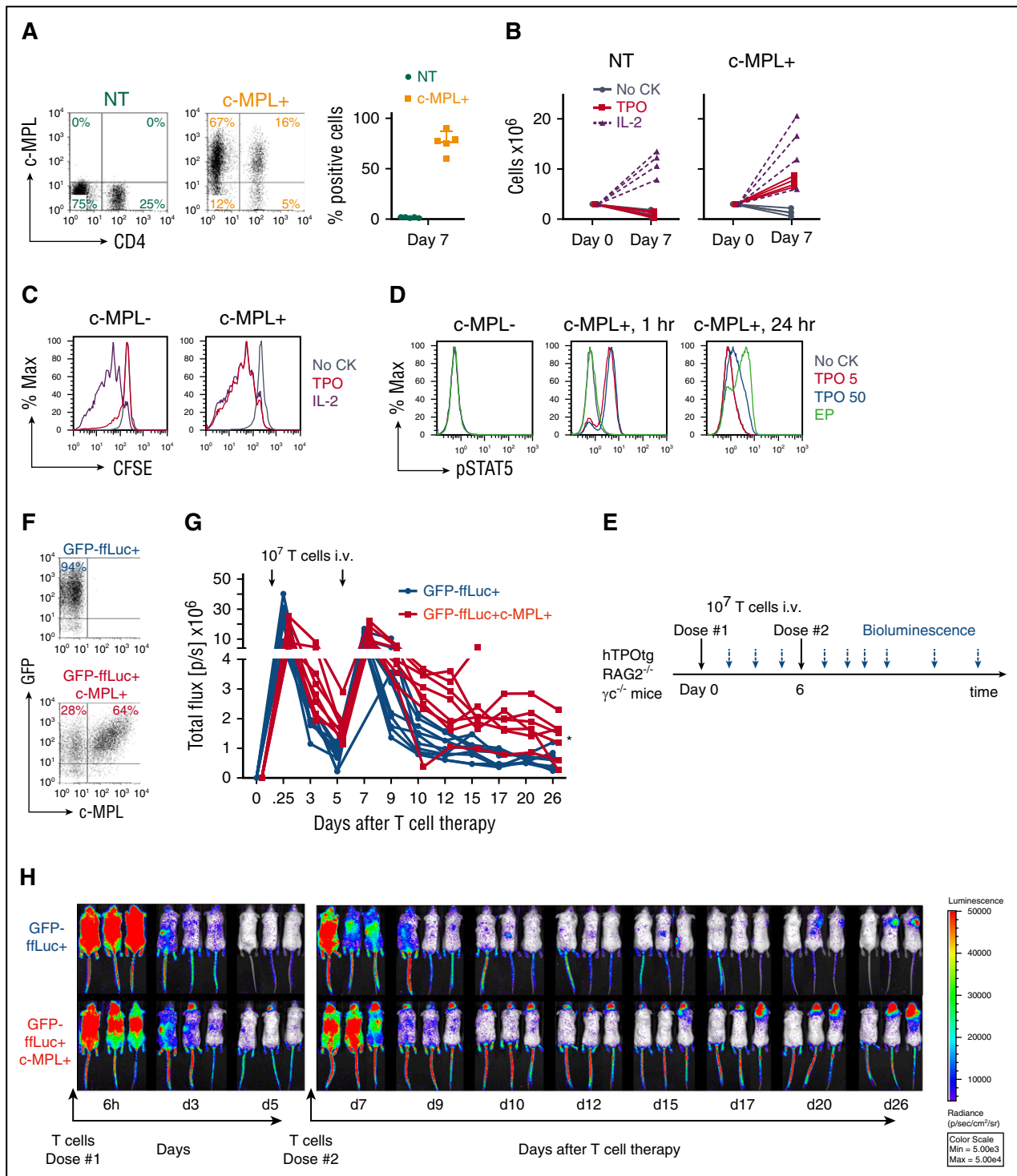
Figure 1. c-MPL expression in polyclonal human T cells produces agonist-dependent proliferation and increased persistence in vivo. (A) c-MPL expression in polyclonal CD4+ and CD8+ T cells 7 days after retroviral transduction, representative FACS plots (left) and summary (right, n = 5). NT, green circles; c-MPL-transduced (c-MPL+), orange squares, mean± SD. (B) Expansion of NT (left) or c-MPL+ (right) T cells cultured in noCK (gray circles, solid lines), TPO 50 ng/mL (red squares, solid lines), or IL-2 50 U/mL (purple triangles, dashed lines) for 7 days. Replicates for n = 4 donors. (C) CFSE dilution of c-MPL-transduced cells cultured in noCK (gray), TPO50 ng/mL (red), or IL-2 50 U/mL (purple) for 7 days, gated on c-MPL⁻ (left) or c-MPL⁺ (right) cells. One representative of 3 donors. (D) c-MPL ligand induced STAT5 phosphorylation in c-MPL⁺ T cells after treatment of 1 or 24 hours with noCK (gray), TPO 5 ng/mL (red), TPO 50 ng/mL (blue) or eltrombopag (EP 0.1 μg/mL, green). (E) Mouse model experimental set up. (F) Transduction efficiency of T cells transduced with GFP-ffLuc alone (top) or cotransduced with GFP-ffLuc and c-MPL (lower) and injected IV into unconditioned hTPOtg-RAG2⁻/⁻γc⁻/⁻ mice. (G) Summary of bioluminescent imaging data of control T cells (GFP-ffLuc⁺, blue circles and lines; n = 10) or c-MPL⁺ T cells (GFP-ffLuc⁺c-MPL⁺, red squares and lines; n = 8). *P = .0003, GFP-ffLuc⁺ vs GFP-ffLuc⁺c-MPL⁺, Student t test on log area under the curve for second T-cell infusion. Combined results from 2 independent experiments. (H) Three representative mice/group imaged over time by BLI; color scale 5 × 10³ to 5 × 10⁴ p/sec/cm²/sr (radiance).
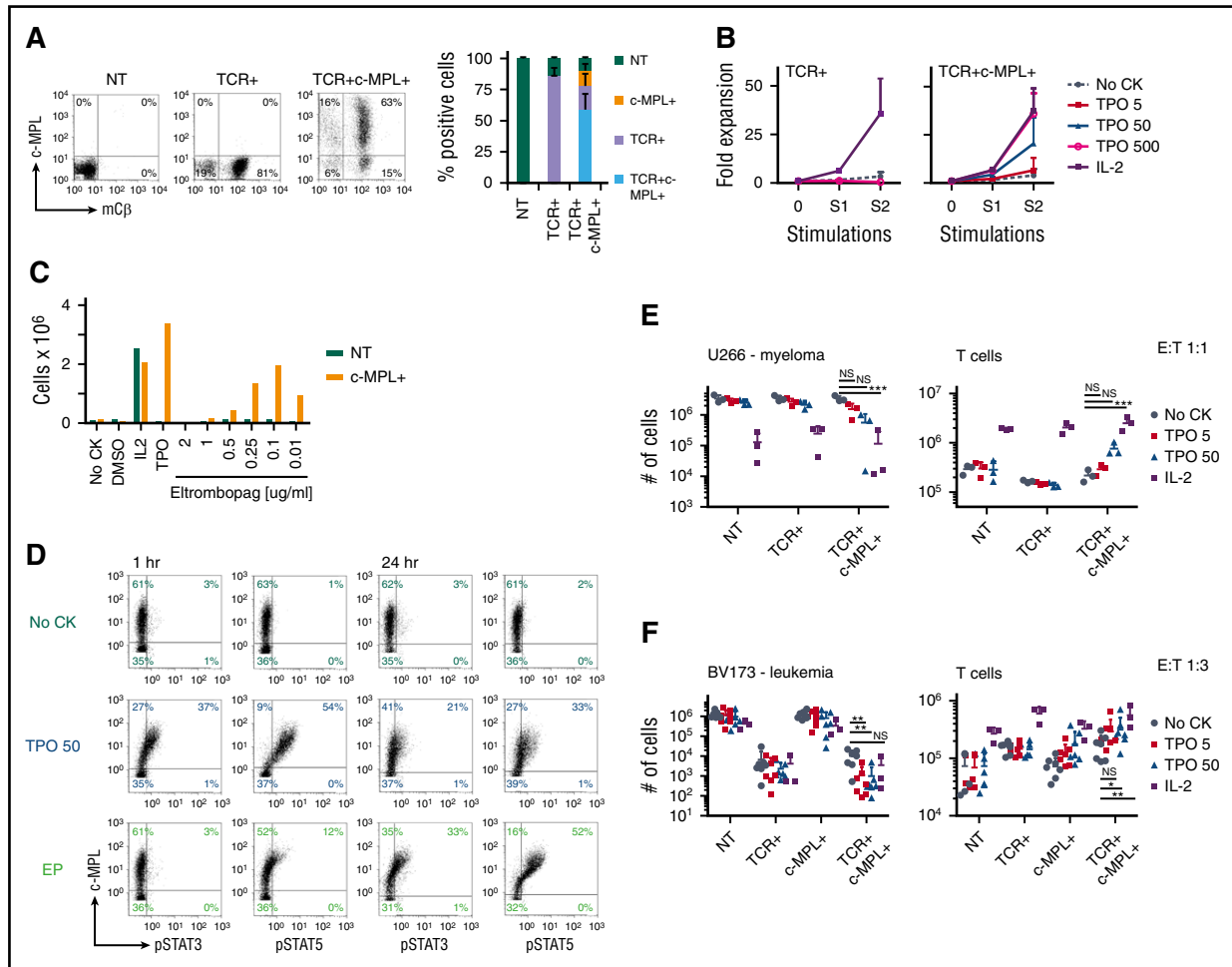
Figure 2. c-MPL is functional in survivin-specific TCR-transgenic T cells and enhances antitumor function in vitro. (A) Transduction efficiencies of CD8^{+} activated T cells with survivin-TCR alone (murine constant β chain, mCβ) or in combination with c-MPL. Representative FACS plots (left) and summary (right), n = 13; mean ± SD. (B) TCR[+]c-MPL^{+} T cells expand upon stimulation with survivin peptide pulsed artificial antigen-presenting cells in a TPO dose-responsive manner (right). TCR^{+} T cells only expand in IL-2, but not high-dose TPO (left, n = 6), except for noCK condition (n = 3; mean ± SD). TCR^{+} T cells at end S2: noCK vs IL-2, P = .003; noCK vs TPO500, P = NS. TCR[+]c-MPL^{+} T cells at end S2: noCK vs IL-2, $P <$ .001; noCK vs TPO5, P = NS; noCK vs TPO50, P = .02; noCK vs TPO500, $P <$ .001; IL-2 vs TPO500, P = NS; Student t test. (C) c-MPL^{+} T cells expand in eltrombopag in a dose-responsive manner during activation with OKT3 and CD28 antibodies, NT T cells only expand in IL-2 50 U/mL, analyzed on day 7. One representative of 3 donors. (D) c-MPL ligand (TPO or EP) induced phosphorylation of STAT3 and STAT5 at 1 hour (left) and 24 hours (right). (E) Coculture of expanded NT, TCR[+], or TCR[+]c-MPL^{+} T cells with U266 myeloma cells (HLA-A*0201[+]survivin[+]) in noCK (gray circles), TPO 5 ng/mL (red squares), TPO 50 ng/mL (blue triangles), or IL-2 25 U/mL (purple squares); effector:target ratio, E:T 1:1. Residual U266 cells (left) and T cells (right) were quantified by FACS on day 5; n = 3; mean ± SD. (F) Coculture with BV173 leukemia cells (HLA-A*0201[+]survivin[+]), E:T 1:3. Residual BV173 cells (left) and T cells (right) were quantified by FACS on day 5; n = 7 for noCK, TPO5, and TPO50; n = 3 for IL-2; mean ± SD. (E, F) *$P <$ .05, **$P <$ .01, ***$P <$ .001, Student t test on log transformed data. NS, not significant.

control T cells (GFP-ffLuc[+] [n = 10] vs GFP-ffLuc[+]c-MPL[+] [n = 8]; P =. 0003, Student t test on log AUC for second T-cell infusion), suggesting that c-MPL^{+} T cells received in vivo homeostatic cytokine signals in the presence of steady-state low systemic TPO levels (Figure 1G-H). Human T-cell persistence was detected in peripheral blood of 2/10 control mice and in 8/8 c-MPL[+] T cell-infused mice on days 15 to 17 (supplemental Figure 3A-B).

c-MPL in tumor-targeted TCR-transgenic T cells provides agonist-dependent enhancement of antitumor function in vitro

We modified our previously described survivin-specific TCR-transgenic T cells with c-MPL to assess agonist-dependent T-cell expansion and enhanced antitumor function.[15] CD8^{+}-selected activated T cells were left NT, single transduced with the survivin-TCR (supplemental Figure 1B), or cotransduced with the survivin-TCR and c-MPL vectors (supplemental Figure 1A-B). Transductions were

highly efficient (Figure 2A), resulting in 58.9 ± 12.6% TCR[+]c-MPL[+], 19.1 ± 9.7% TCR[+]c-MPL[−], and 12.1 ± 5.5% TCR[−]c-MPL^{+} cells in the cotransduced group and 86.1 ± 6.3% TCR^{+} cells in the TCR[+] group (mean ± SD; n = 13; Figure 2). Next, we tested whether rhTPO supports antigen-specific T-cell expansion of TCR[+]c-MPL^{+} T cells by stimulating TCR[+] or TCR[+]c-MPL^{+} T cells with irradiated survivin peptide-pulsed artificial antigen-presenting cells in the presence of increasing concentrations of rhTPO (Figure 2B). TCR^{+} T cells expanded in the presence of IL-2 but not in rhTPO, even in very high concentrations (500 ng/mL), or in the absence of cytokines (Figure 2B). In contrast, TCR[+]c-MPL^{+} T cells readily expanded in a TPO-dose-dependent manner (Figure 2B) with comparable expansion levels to cells cultured in IL-2.

We obtained similar results with the TPO small molecule agonist EP. We used a dose-titration experiment to determine the optimal concentration of EP to support c-MPL[+] T-cell expansion (Figure 2C). EP was previously shown to inhibit leukemia cell proliferation at
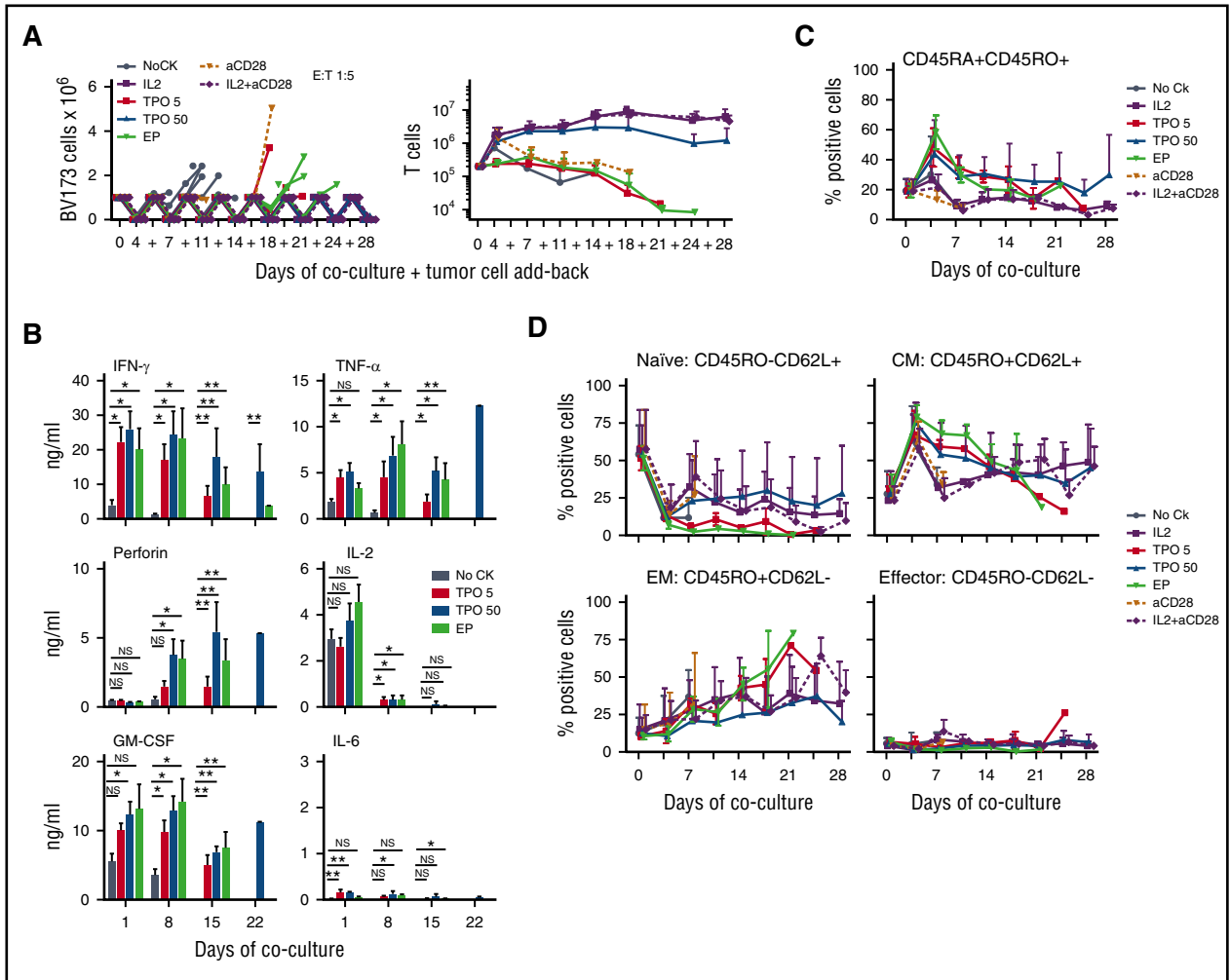
Figure 3. Ligand-induced c-MPL activation supports sequential killing activity and T-cell expansion in TCR-transgenic T cells. (A) Serial coculture with BV173 leukemia cells, E:T 1:5. Residual BV173 cells (left) and T cells (right) were quantified by FACS every 3 to 4 days from a total of 8 replicate wells per donor, and BV173 cells were added-back to untouched wells (+) at each point. Cultures in noCK (gray circles), IL-2 25 U/mL (purple squares), TPO 5 ng/mL (red squares), TPO 50 ng/mL (blue triangles), EP 0.1 μg/mL (green triangles), plate-bound anti-CD28 (orange triangles, dotted line), IL-2 (25 U/mL) + plate-bound anti-CD28 (purple diamond, dotted line); n = 3 for IL-2, anti-CD28, IL-2+anti-CD28, TPO5, EP; n = 6 for noCK, TPO50. Lines of individual donors are shown for tumor cell counts; mean ±SD for T-cell counts. (Left) Serial killing activity was analyzed by Kaplan-Meier analysis: overall, $P < .0001$; noCK vs TPO5, $P = .007$; noCK vs TPO50, $P < .0001$; noCK vs EP, $P = .003$; noCK vs IL-2, $P < .0001$; noCK vs aCD28, $P = .038$; noCK vs aCD28+IL-2, $P < .0001$. TPO50 vs IL-2, $P = $ NS; TPO50 vs aCD28, $P = .003$; TPO50 vs aCD28+IL-2, $P = $ NS. (Right) T-cell expansion in noCK vs TPO5, $P = $ NS; noCK vs TPO50, $P = .003$; noCK vs EP, $P = $ NS; noCK vs IL-2, $P = .001$; noCK vs aCD28, $P = $ NS; noCK vs aCD28+IL-2, $P = .001$. TPO5 vs TPO50, $P = .02$; TPO5 vs EP, $P = $ NS; TPO50 vs EP, $P = .03$; TPO50 vs IL-2, $P = $ NS; TPO50 vs aCD28+IL-2, $P = $ NS. Student t test on log area under the curve. (B) Cytokine levels in coculture supernatants 24 hours after tumor cell challenge for the first, third, fifth, and seventh tumor challenge on days 1, 8, 15, and 22 of coculture, respectively; n = 3; mean ± SD, analyzed in duplicates. Student t test on log transformed data (days 1, 8), 1 sample Student t test compares with null hypothesis of 0 on log transformed data (days 15, 22). *$P < .05$, **$P < .01$. (C-D) T-cell phenotype of CD3+CD8+TCR+c-MPL+ T cells recovered from cocultures at each time-point; n = 3-6 (as in A); mean ± SD. (C) Percentages of CD45RA+CD45RO+ cells. No Ck vs TPO5, $P = .002$; noCK vs TPO50, $P < .0001$; noCK vs EP, $P = .002$; noCK vs IL-2, $P = .002$; noCK vs aCD28, $P = $ NS; noCK vs aCD28+IL-2, $P = .004$. TPO50 vs IL-2, $P = .05$; TPO50 vs aCD28, $P < .0001$; TPO50 vs aCD28+IL-2, $P = .005$. Student t test on log area under the curve. (D) Naïve, central memory (CM), effector memory (EM), and effector T cells. Naïve: $P = $ NS, except noCK vs TPO50, $P = .05$; noCK vs aCD28+IL-2, $P = .05$; CM: noCK vs TPO5, $P = .003$; noCK vs TPO50, $P < .0001$; noCK vs EP, $P = .002$; noCK vs IL-2, $P = .005$; noCK vs aCD28, $P = $ NS; noCK vs aCD28+IL-2, $P = .009$. TPO50 vs IL-2, $P = $ NS; TPO50 vs aCD28, $P = .001$, TPO50 vs aCD28+IL-2, $P = .03$. EP vs aCD28+IL-2, $P = .04$; Student t test on log area under the curve day 14.

higher concentrations (1-10 μg/mL) by reduction of intracellular iron, a c-MPL-independent effect.[18] NT or c-MPL+ T cells were re-activated on OKT3/CD28-coated plates in the presence of different EP concentrations, and expansion of viable T cells was determined after 7 days. An EP concentration of 0.1 μg/mL was retained for further in vitro studies, as higher levels were toxic to the T cells and lower levels did not show c-MPL-dependent effects. Thus, the effective EP concentration for c-MPL+ T cells was about 1 log lower than in previous reports assessing effects of EP on megakaryocytic progenitor cells or leukemia cells.[18,19] To assess c-MPL ligand-dependent signaling in TCR+c-MPL+ T cells, cells were left untreated (no cytokine [noCK]) or treated with TPO50 or EP for

1 or 24 hours. Only c-MPL+ cells phosphorylated STAT3 and STAT5 after treatment with rhTPO or EP, whereas c-MPL− cells did not, and EP treatment mostly led to JAK/STAT activation in c-MPL high expressing cells (Figure 2D). Next, we evaluated whether rhTPO enhanced the antitumor function of TCR+c-MPL+ T cells using 2 different HLA-A*0201+survivin+ hematologic malignancies as targets (U266 multiple myeloma, BV173 leukemia; Figure 2E-F). Addition of rhTPO at 50 ng/mL to the cocultures showed a trend toward enhanced killing of U266 cells (left) and enhanced persistence of TCR+c-MPL+ T cells (right) compared with noCK controls (Figure 2E). Addition of IL-2 25U/mL, however, led to substantial enhancement of antigen-independent tumor cell killing and T-cell expansion (U266 with
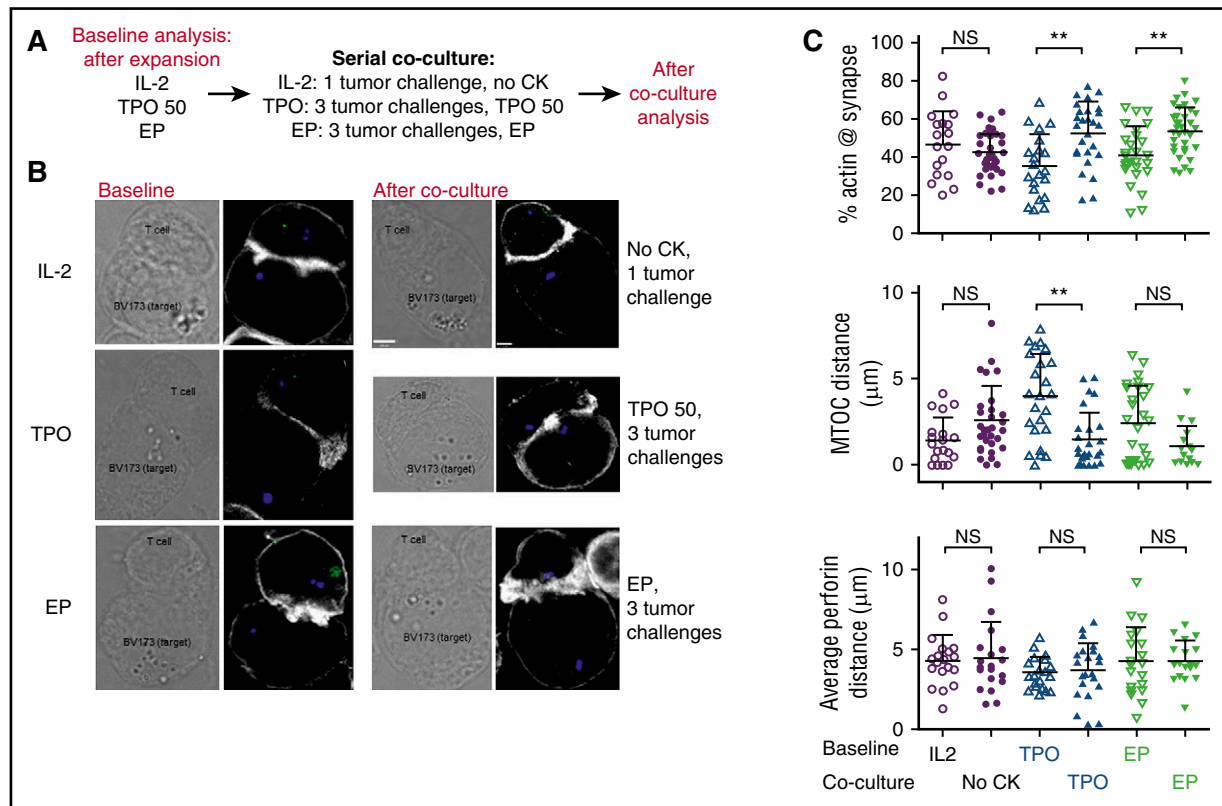
Figure 4. c-MPL stimulated sequential killer T cells form more efficient immune synapses. (A) Experimental set up. (B) Representative images of immune synapses between T cells and BV173 leukemia cells. Phase contrast (left) and confocal images (right) at baseline and after coculture. Actin (white), pericentrin (blue), perforin (green). (C) Quantification of the percentage actin at the synapse, the distance of the microtubule organization center to the synapse, and the perforin distance to the synapse. n = 3, mean ± SD. **$P \leq .01$; Student t test on log transformed data. NS, not significant.

TCR$^+$c-MPL$^+$ T cells: noCK vs TPO50 43.3 ± 1.1 × 10^5 vs 22.8 ± 11.2 × 10^5 [$P = .17$]; noCK vs IL-2 43.3 ± 1.1 × 10^5 vs 3.13 ± 0.45 × 10^5 [$P < .0001$]; T-cell count: noCK vs TPO50 1.84 ± 0.31 × 10^5 vs 4.41 ± 5.11 × 10^5 [$P = .59$]; noCK vs IL-2 1.84 ± 0.31 × 10^5 vs 25.2 ± 7.2 × 10^5 [$P = .0002$]; n = 3; mean ± SD). We obtained significantly enhanced killing of tumor cells in the presence of rhTPO at 50 ng/mL in the BV173 leukemia cocultures (Figure 2F; BV173 with TCR$^+$c-MPL$^+$ T cells: noCK vs TPO50 10.3 ± 7.9 × 10^3 vs 0.99 ± 1.7 × 10^3 [$P = .002$]; noCK vs IL-2 10.3 ± 7.9 × 10^3 vs 3.52 ± 5.27 × 10^3 [$P = .13$]; T-cell count: noCK vs TPO50 16.7 ± 8.1 × 10^4 vs 31.5 ± 19.1 × 10^4 [$P = .05$]; noCK vs IL-2 16.7 ± 8.1 × 10^4 vs 56.2 ± 25.2 × 10^4 [$P = .006$]; n = 7 for noCK, TPO5, and TPO50; n = 3 for IL-2; mean ± SD). Again, addition of IL-2 led to significant but antigen-independent enhancement of T-cell expansion.

c-MPL activation enables sequential killing activity and expansion of central memory TCR$^+$c-MPL$^+$ T cells

To study the effects of c-MPL signaling in TCR$^+$ T cells in the presence of high tumor load, T cells were transduced with a polycistronic vector expressing both the TCR and c-MPL in a single construct (supplemental Figure 1C). Viral copy number per cell was 4.87 ± 2.48 copies (n = 3; mean ± SD; supplemental Figure 1D). We added TCR$^+$c-MPL$^+$ T cells to BV173 leukemia cells and added these target cells back every 3 to 4 days to culture replicate wells up to 8 times (Figure 3A). TCR$^+$c-MPL$^+$ T cells in the absence of cytokines or with plate-bound anti-CD28 alone killed only 1 to 2 times, whereas addition of rhTPO, EP, IL-2, or plate-bound anti-CD28+IL-2 significantly increased the repetitive killing capacity of the cells up to 8 times

(Figure 3A, left), and also significantly enhanced T cell expansion (Figure 3A, right). Time to cell killing was analyzed by Kaplan-Meier analysis and revealed consistent outcomes (overall $P < .0001$). In addition, both rhTPO and EP sustained the levels of Th1 cytokine production in sequential cocultures (Figure 3B). Importantly, c-MPL stimulated sequential killer T cells did not show signs of growth factor-independent T-cell growth after withdrawal of antigen and c-MPL stimulation (supplemental Figure 4). Persistent T cells were also analyzed for memory T-cell markers over time. T cells cocultured in rhTPO or EP showed enrichment in CD45RA$^+$CD45RO$^+$ (Figure 3C) and central memory cells (Figure 3D) with lower proportions of effector memory cells. Naive cells were enriched in some of the donors, but donor to donor variability was high (Figure 3D).

Immune synapse formation is more efficient in T cells with c-MPL activation

To analyze immune synapse formation between TCR$^+$c-MPL$^+$ T cells and BV173 leukemia target cells, we performed confocal microscopy and compared synapses formed under baseline conditions after T-cell expansion to synapses formed from T cells purified after cocultures (Figure 4). In the absence of c-MPL activation, T cells were isolated after a single tumor cell challenge because these T cells do not kill repetitively and do not survive 3 tumor cell challenges. We did not detect increased actin accumulation at the synapse (baseline vs coculture 46.2 ± 17.4% vs 42.2 ± 10.9%; mean ± SD; $P = $ NS), shortening of the distance from the microtubule organization center to the synapse (MTOC distance, baseline vs coculture 1.42 ± 1.32 μm vs 2.57 ± 2.02 μm; mean ± SD; $P = $ NS), or perforin convergence in
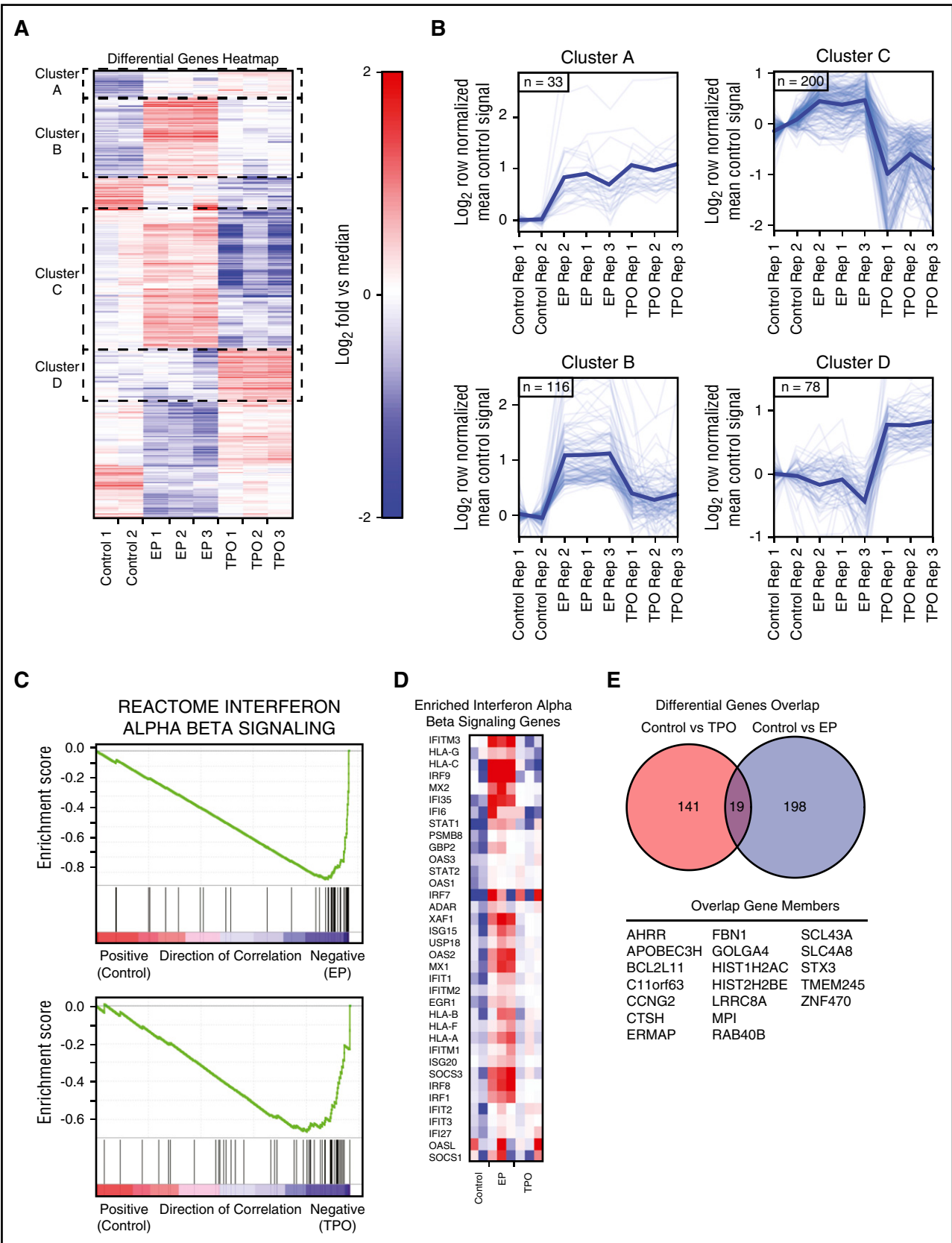
Figure 5. c-MPL signaling in tumor-targeted TCR-transgenic T cells is immune stimulatory. (A) Heat map of median normalized differential gene expression clustered by overall expression behavior. (B) Control signal mean normalized expression behavior of highlighted clusters from heat map. (C) Gene set enrichment analysis output for reactome interferon α β signaling gene set showing correlation between control and EP treatment, and control and TPO treatment. (D) Heat map of enriched genes in interferon α β signaling genes. (E) Genes in the overlap of the control vs EP and control vs TPO differential genes.

Figure 6. c-MPL signaling in T cells significantly enhances antitumor function in a leukemia xenograft model. (A) Experimental set up. (B) Kaplan-Meier survival analysis. Survival of hTPOtg-RAG2$^{-/-}$γc$^{-/-}$ mice, injected with BV173-ffLuc$^+$ cells and treated with control T cells (n = 7), TCR$^+$ T cells (n = 9), TCR$^+$c-MPL$^+$ T cells and PBS injections (n = 14), TCR$^+$c-MPL$^+$ T cells and rhTPO injections (n = 10). Results combined from 3 independent experiments. Overall survival: P = .004. TCR vs TCR$^+$c-MPL$^+$ (PBS injected): P = .27. TCR vs TCR$^+$c-MPL$^+$ (rhTPO injected): P = .001. TCR$^+$c-MPL$^+$ (PBS injected) vs TCR$^+$c-MPL$^+$ (rhTPO injected): P = .07. (C) 3 representative mice/group imaged over time by BLI; color scale 5 × 10^3 to 5 × 10^4 p/sec/cm^2/sr. (D) Summary of BLI data by treatment condition, results combined from 3 independent experiments, mean ± SD. Control T cells (n = 7, lime green circles solid lines), TCR$^+$ T cells (n = 9, lavender squares solid lines), TCR$^+$c-MPL$^+$ T cells (PBS injected; n = 14, blue triangles up solid lines), TCR$^+$c-MPL$^+$ T cells (rhTPO injected; n = 10, blue triangles down dotted lines). TCR vs TCR$^+$c-MPL$^+$ (PBS injected): P = .004. TCR vs TCR$^+$c-MPL$^+$ (rhTPO injected): P = .0005. TCR$^+$c-MPL$^+$ (PBS injected) vs TCR$^+$c-MPL$^+$ (rhTPO injected): P = .088. Statistics was performed using the Student t test on log AUC at week 4 compared with week 1.

TCR$^+$c-MPL$^+$ T cells reisolated after 1 BV173 challenge (baseline vs coculture 4.30 ± 1.59 μm vs 4.47 ± 2.27 μm; mean ± SD; P = NS). To analyze the immune synapses formed by c-MPL stimulated sequential killer T cells, TCR$^+$c-MPL$^+$ T cells were reisolated after 3 tumor cell challenges in the presence of rhTPO or EP. Both rhTPO- or EP-stimulated cells showed significantly increased actin accumulation at the synapse (TPO baseline vs coculture 35.23 ± 16.41% vs 52.60 ± 16.32%; mean ± SD; P = .001; EP baseline vs coculture 40.95 ± 14.82% vs 53.29 ± 12.47%; mean ± SD; P = .003) and shortening of the MTOC to synapse distance (TPO MTOC distance, baseline vs coculture 3.96 ± 2.49 μm vs 1.46 ± 1.58 μm; mean ± SD; P = .01; EP MTOC distance, baseline vs coculture 2.42 ± 2.16 μm vs 1.09 ± 1.16 μm; mean ± S; P = NS), indicating the formation of more efficient cytotoxic immune synapses in the presence of c-MPL signaling. Perforin convergence was unchanged regardless of c-MPL signaling (TPO baseline vs coculture 3.53 ± 1.00 μm vs 3.68 ± 1.70 μm; mean ± SD; P = NS; EP baseline vs coculture 4.26 ± 2.08 μm vs 4.25 ± 1.28 μm; mean ± SD; P = NS).

c-MPL signaling produces immune stimulation in TCR-transgenic sequential killer T cells

To study the molecular pathways affected by rhTPO- or EP-mediated c-MPL signaling in TCR-transgenic T cells during tumor cell killing, we analyzed the gene expression profiles of c-MPL enabled sequential killer T cells compared with TCR$^+$c-MPL$^+$ T cells in the absence

of c-MPL activation (Figure 5). Analogous to the experimental set-up of the synapse imaging studies, TCR$^+$c-MPL$^+$ T cells were subjected to multiple rounds of coculture with BV173 leukemia cells, and RNA was isolated from purified surviving T cells after 1 tumor cell challenge for the control condition (coculture in the absence of exogenous cytokines), or after 3 BV173 challenges in the presence of rhTPO or EP. The heat map of differentially expressed genes led to the identification of 2 clusters with coherent upregulation of genes (clusters A and B) and 2 clusters with differentially regulated genes (clusters C and D) in cocultured cells exposed to rhTPO or EP (Figure 5A-B; supplemental Table 1). Gene set enrichment analysis identified the IFN-α/β signaling pathway as the single most highly upregulated pathway in c-MPL stimulated cocultures (Figure 5C-D) and cell cycle associated genes as significantly differentially expressed in rhTPO vs EP treatment conditions (supplemental Figure 5). Cell cycle associated genes were upregulated in T cells from EP-treated cocultures vs controls and downregulated in T cells from rhTPO-treated cocultures vs controls or EP-treatment, suggesting that during coculture with tumor targets EP has a significant c-MPL-independent effect on cell cycle genes (supplemental Figure 5).

c-MPL signaling in TCR-transgenic T cells enhances antitumor function in vivo

To test the in vivo antitumor function of TCR$^+$c-MPL$^+$ T cells in a mouse leukemia xenograft model, we adapted our previously described

model[15] to hTPOtg-RAG2$^{-/-}\gamma$c$^{-/-}$ mice. To "stress" this system and better detect the effects of human TPO on TCR$^+$c-MPL$^+$ T cells, we gave the same dose of 3×10^6 BV173-ffLuc tumor cells to sublethally irradiated mice,[15] but reduced the administered T-cell dose from 3 infusions of 10×10^6 cells to a single infusion of 5×10^6 cells, and omitted systemic T-cell support with IL-2 injections postinfusion (Figure 6A). To analyze homeostatic effects of TPO on transgenic T cells, mice receiving TCR$^+$c-MPL$^+$ T cells were either treated with daily subcutaneous saline (phosphate-buffered saline) or with daily subcutaneous rhTPO (50 μg/kg/mouse) injections for the first 28 days. Groups of mice were compared with mice receiving TCR$^+$ T cells alone, without c-MPL stimulation. We tested whether homeostatic TPO alone or the combination of homeostatic TPO and pharmacologic TPO treatment improved the antileukemic effect of TCR-transgenic T cells. Overall survival was significantly improved in the presence of c-MPL activation ($P = .004$; Figure 6B). Even with a single low dose of TCR$^+$c-MPL$^+$ T cells, we could detect a trend to delayed leukemia growth by BLI in mice with steady-state TPO levels ($P = $ NS) and a significant delay in mice with steady-state TPO levels and rhTPO injections ($P = .001$) compared with TCR$^+$ T cells alone (Figure 6C-D). These results suggest a dose-response effect of c-MPL signaling in transgenic T cells when compared with mice receiving T cells without c-MPL stimulation (TCR$^+$ group).

Discussion

Here we explore whether transgenic expression of the nonlymphoid hematopoietic growth factor receptor c-MPL in TCR-transgenic T cells benefits T-cell survival and function after its activation. We found that c-MPL signaling in T cells activates both costimulatory (signal 2) and cytokine receptor (signal 3) pathways in the presence of TCR signaling, thus leading to significantly enhanced antitumor function, immune synapse formation, cytokine production, and T-cell expansion/survival, all features that are typically suboptimal in TCR-transgenic T cells.

In polyclonal T cells, c-MPL activation leads to TPO-dependent T-cell expansion and proliferation in vitro and to increased persistence in vivo in human TPO transgenic immunodeficient mice. These results illustrate that c-MPL signaling produces a homeostatic cytokine effect in T cells similar to common γ-chain cytokine signaling (such as IL-2), in the absence of TCR activation (signal 1). In addition, this effect is strictly dependent on the cognate ligand, as c-MPL$^+$ T cells do not expand or proliferate in the absence of exogenously added rhTPO. Absence of cell autonomous ligand-independent growth supports the safety of our approach.

In tumor-targeted TCR-transgenic c-MPL$^+$ T cells, c-MPL activation by either rhTPO or the small molecule agonist EP produces dose-dependent T-cell expansion and enhances antitumor function. Indeed, c-MPL signaling enabled TCR$^+$ T cells to sequentially kill tumor cells, improved ligand-dependent Th1 cytokine production and preservation of a central memory phenotype, and had a potent effect on the formation of superior immune synapses. We observed increased actin accumulation at the synapse as well as a better polarization of the MTOC to the synapse in the presence of c-MPL ligand. These components have been identified previously as essential indicators of effective lytic synapse formation in both native cytotoxic cells[20-22] and engineered T cells.[23] Because efficient synapse formation also depends on the presence of several other receptors (eg, adhesion molecules, costimulatory or checkpoint receptors),[24] we conclude that c-MPL activation during TCR stimulation and sequential tumor cell killing

provides additional signals required to produce stronger lytic synapses between engineered T cells and their target cells.

To further analyze the molecular events occurring in c-MPL$^+$ TCR-transgenic cells during sequential cytotoxic activity, we performed an unbiased RNA-seq analysis. We found that c-MPL stimulation upregulates genes in the type 1 interferon (IFN) pathway, providing potent immune-stimulatory signals to the engineered T cells, such as those seen during viral infections.[25] Previously, type 1 IFNs have been shown to potently support cytotoxic T cells by direct or indirect mechanisms during viral infection, and also to enhance anticancer immunity.[26,27] In addition, type 1 IFNs increase the expression of perforin or granzyme B in cytotoxic T cells and promote the survival of memory T cells, and we observed both in our study. These findings, together with the fact that c-MPL signaling activates multiple known cellular pathways that are shared by classical T-cell costimulatory and cytokine receptors,[5,13,14] support our conclusion that c-MPL signaling in T cells can simultaneously produce both beneficial signals 2 and 3 in engineered T cells.

Although many of the c-MPL-dependent gene expression changes were observed in both the TPO and EP treatment groups, we also found significant differences between genes expressed in response to each stimulus. TPO-treated sequential killer T cells downregulated cell cycle, growth, or proliferation signatures, whereas these pathways were upregulated in the EP-treated T cells. We attribute this finding to the fact that EP treatment can also have significant c-MPL-independent effects on cells, as previously shown in acute myeloid leukemia cells.[18,28,29] In gene expression studies performed on HL-60 AML cells treated with EP at 3 μg/mL, EP treatment led to downregulation of cell cycle-associated genes with a block in the G1 phase of cell cycle.[18] Although we found that EP treatment at 3 μg/mL was uniformly lethal to T cells, EP treatment at 0.1 μg/mL supported sequential killing by engineered T cells and significantly enhanced cell cycle and proliferation-associated gene signatures. These results demonstrate the striking dose-dependent effects of EP on T-cell cycle and proliferation pathways. In contrast, treatment of engineered T cells with rhTPO led to down-regulation of cell cycle and proliferation pathways compared with controls or EP treated cells, consistent with the known ability of TPO-signaling in HSCs to induce quiescence and maintenance of the HSC pool.[5]

TPO is produced not only systemically in the liver and kidneys but also locally in the BM microenvironment by cells of the hematopoietic stem cell niche, such as stroma cells or osteoblasts, and also by malignant myeloid blasts.[9,30] TPO is required for the maintenance of the HSC pool as it promotes HSC self-renewal and expansion in vivo, but can also induce HSC quiescence, a state critical to stem cell reservoir maintenance and avoiding premature exhaustion.[5] In adoptively transferred T cells, a less differentiated phenotype is desirable, as these cells tend to persist longer in the host.[31-33] In addition, TPO levels are significantly higher in BM than serum in steady-state, and are substantially increased during chemotherapy-induced thrombocytopenia,[34] in leukemic BM[35] and in a mouse model of myeloproliferative disease.[10] In that mouse model, elevated BM TPO levels contributed significantly to the remodeling of a self-reinforcing leukemic stem cell niche that promoted progression of myeloproliferative disease.[10] c-MPL is therefore well suited for enhancing TCR-transgenic T-cell activity against hematological malignancies, as there are at least 5 possible means by which benefit could be produced in vivo: (1) systemic low TPO serum levels mediate homeostatic cytokine signals, (2) local high TPO levels in the malignant BM microenvironment support local tumor-specific T-cell expansion, (3) T cells with high c-MPL expression scavenge TPO from the tumor microenvironment and

deprive leukemic blasts of the TPO signaling required for their survival, (4) administration of MPL-agonist drugs electively enhances transgenic T-cell function, and (5) the window of postchemotherapy thrombocytopenia accompanied by high serum TPO levels could be exploited for T-cell infusion. In vivo, in our human TPO-transgenic immunodeficient leukemia xenograft mouse model, we demonstrate that steady-state TPO exerts a homeostatic cytokine effect on transferred c-MPL+ TCR-transgenic T cells by slowing down leukemia progression. The combination of steady-state homeostatic TPO levels and pharmacologic dosing of rhTPO achieved the best result compared with mice receiving T cells in the absence of c-MPL activation (TCR+ group). Our results provide a proof of concept that transgenic c-MPL in T cells can respond to either a soluble bone marrow microenvironment factor TPO or a receptor agonist drug (rhTPO).

Given the multiplicity of activities associated with forced expression of c-MPL, we propose that our approach could be used in a number of clinical settings. Transgenic c-MPL+survivin-TCR+ T cells could be valuable for survivin+HLA-A2+ myeloid malignancies (c-MPL+ T cells would lead to deprivation of TPO from the BM) and for survivin+HLA-A2+ lymphoid malignancies (c-MPL+ T cells benefit from endogenous TPO levels, c-MPL agonist drugs could be used to support transgenic T-cell function).

In conclusion, we suggest this novel immuno-therapeutic strategy to enhance the function and persistence of tumor-targeted TCR-engineered T cells with transgenic expression of the hematopoietic growth factor receptor c-MPL will be able to augment the antitumor activity of transgenic T cells by activation of both costimulatory and cytokine pathways, including type 1 IFN.

Acknowledgments

Authorship

Contribution: C.D.N. performed experiments, analyzed and interpreted results, and edited the manuscript; M.M. and D.A.B. performed confocal microscopy and analyzed and interpreted results; R.A.H. and C.Y.L. analyzed and interpreted RNA-seq data; D.A.B. and L.O. performed experiments; M.-F.W. and H.L. analyzed results and performed statistics; O.D. determined viral copy numbers by quantitative PCR; J.S.O. provided microscopy infrastructure and reagents for synapse studies; M.K.B. discussed study design and results and edited the manuscript; C.A. designed the study, performed experiments, analyzed and interpreted results, and wrote the manuscript; and all authors reviewed and approved the final version of the manuscript.

Conflict-of-interest disclosure: C.Y.L. receives royalty payments from Syros Pharmaceuticals and has sponsored travel from Novartis Institute for Biomedical Research; C.A. receives royalty payments from Cell Medica. The remaining authors declare no competing financial interest.

The current affiliation for C.A. is Department of Oncology, Centre Hospitalier Universitaire Vaudois, University of Lausanne, Ludwig Institute for Cancer Research, Lausanne Branch, Epalinges, Switzerland.

Correspondence: Caroline Arber, Department of Oncology, Centre Hospitalier Universitaire Vaudois, University of Lausanne, Ludwig Institute for Cancer Research, Lausanne Branch, Chemin des Boveresses 155, CH-1066 Epalinges, Switzerland; e-mail: caroline.arber@unil.ch or caroline.arber-barth@chuv.ch.

References

1. Kershaw MH, Westwood JA, Darcy PK. Gene-engineered T cells for cancer therapy. Nat Rev Cancer. 2013;13(8):525-541.

2. Fesnak AD, June CH, Levine BL. Engineered T cells: the promise and challenges of cancer immunotherapy. Nat Rev Cancer. 2016;16(9):566-581.

3. Cheever MA, Allison JP, Ferris AS, et al. The prioritization of cancer antigens: a national cancer institute pilot project for the acceleration of translational research. Clin Cancer Res. 2009;15(17):5323-5337.

4. Dotti G, Gottschalk S, Savoldo B, Brenner MK. Design and development of therapies using chimeric antigen receptor-expressing T cells. Immunol Rev. 2014;257(1):107-126.

5. Hitchcock IS, Kaushansky K. Thrombopoietin from beginning to end. Br J Haematol. 2014;165(2):259-268.

6. Kaushansky K, Lok S, Holly RD, et al. Promotion of megakaryocyte progenitor expansion and differentiation by the c-Mpl ligand thrombopoietin. Nature. 1994;369(6481):568-571.

7. Fox N, Priestley G, Papayannopoulou T, Kaushansky K. Thrombopoietin expands hematopoietic stem cells after transplantation. J Clin Invest. 2002;110(3):389-394.

8. Qian H, Buza-Vidas N, Hyland CD, et al. Critical role of thrombopoietin in maintaining adult quiescent hematopoietic stem cells. Cell Stem Cell. 2007;1(6):671-684.

9. Yoshihara H, Arai F, Hosokawa K, et al. Thrombopoietin/MPL signaling regulates hematopoietic stem cell quiescence and interaction with the osteoblastic niche. Cell Stem Cell. 2007;1(6):685-697.

10. Schepers K, Pietras EM, Reynaud D, et al. Myeloproliferative neoplasia remodels the endosteal bone marrow niche into a self-reinforcing leukemic niche. Cell Stem Cell. 2013;13(3):285-299.

11. Chang M, Suen Y, Meng G, et al. Differential mechanisms in the regulation of endogenous levels of thrombopoietin and interleukin-11 during thrombocytopenia: insight into the regulation of platelet production. Blood. 1996;88(9):3354-3362.

12. Grozovsky R, Begonja AJ, Liu K, et al. The Ashwell-Morell receptor regulates hepatic thrombopoietin production via JAK2-STAT3 signaling. Nat Med. 2015;21(1):47-54.

13. Chen L, Flies DB. Molecular mechanisms of T cell co-stimulation and co-inhibition. Nat Rev Immunol. 2013;13(4):227-242.

14. Rochman Y, Spolski R, Leonard WJ. New insights into the regulation of T cells by gamma(c) family cytokines. Nat Rev Immunol. 2009;9(7):480-490.

15. Arber C, Feng X, Abhyankar H, et al. Survivin-specific T cell receptor targets tumor but not T cells. J Clin Invest. 2015;125(1):157-168.

16. Quintarelli C, Dotti G, De Angelis B, et al. Cytotoxic T lymphocytes directed to the preferentially expressed antigen of melanoma (PRAME) target chronic myeloid leukemia. Blood. 2008;112(5):1876-1885.

17. Rongvaux A, Willinger T, Takizawa H, et al. Human thrombopoietin knockin mice efficiently support human hematopoiesis in vivo. Proc Natl Acad Sci USA. 2011;108(6):2378-2383.

18. Roth M, Will B, Simkin G, et al. Eltrombopag inhibits the proliferation of leukemia cells via reduction of intracellular iron and induction of differentiation. *Blood*. 2012;120(2):386-394.

19. Will B, Kawahara M, Luciano JP, et al. Effect of the nonpeptide thrombopoietin receptor agonist Eltrombopag on bone marrow cells from patients with acute myeloid leukemia and myelodysplastic syndrome. *Blood*. 2009;114(18):3899-3908.

20. Grakoui A, Bromley SK, Sumen C, et al. Pillars article: The immunological synapse: a molecular machine controlling T cell activation. Science. 1999. 285: 221-227. *J Immunol*. 2015;194(9): 4066-4072.

21. Monks CR, Freiberg BA, Kupfer H, Sciaky N, Kupfer A. Pillars article: Three-dimensional segregation of supramolecular activation clusters in T cells. Nature. 1998. 395: 82-86. *J Immunol*. 2015;194(9):4061-4065.

22. McGavern DB, Christen U, Oldstone MB. Molecular anatomy of antigen-specific CD8(+) T cell engagement and synapse formation in vivo. *Nat Immunol*. 2002;3(10):918-925.

23. Hegde M, Mukherjee M, Grada Z, et al. Tandem CAR T cells targeting HER2 and IL13Rα2 mitigate tumor antigen escape. *J Clin Invest*. 2016;126(8):3036-3052.

24. Dustin ML. The immunological synapse. *Cancer Immunol Res*. 2014;2(11):1023-1033.

25. Crouse J, Kalinke U, Oxenius A. Regulation of antiviral T cell responses by type I interferons. *Nat Rev Immunol*. 2015;15(4):231-242.

26. Zitvogel L, Galluzzi L, Kepp O, Smyth MJ, Kroemer G. Type I interferons in anticancer immunity. *Nat Rev Immunol*. 2015;15(7):405-414.

27. Zhao Z, Condomines M, van der Stegen SJC, et al. Structural design of engineered costimulation determines tumor rejection kinetics and persistence of CAR T cells. *Cancer Cell*. 2015;28(4):415-428.

28. Sugita M, Kalota A, Gewirtz AM, Carroll M. Eltrombopag inhibition of acute myeloid leukemia cell survival does not depend on c-Mpl expression. *Leukemia*. 2013;27(5): 1207-1210.

29. Kalota A, Selak MA, Garcia-Cid LA, Carroll M. Eltrombopag modulates reactive oxygen species and decreases acute myeloid leukemia cell survival. *PLoS One*. 2015;10(4):e0126691.

30. Corazza F, Hermans C, D'Hondt S, et al. Circulating thrombopoietin as an in vivo growth factor for blast cells in acute myeloid leukemia. *Blood*. 2006;107(6):2525-2530.

31. Gattinoni L, Speiser DE, Lichterfeld M, Bonini C. T memory stem cells in health and disease. *Nat Med*. 2017;23(1):18-27.

32. Sabatino M, Hu J, Sommariva M, et al. Generation of clinical-grade CD19-specific CAR-modified CD8+ memory stem cells for the treatment of human B-cell malignancies. *Blood*. 2016;128(4):519-528.

33. Biasco L, Scala S, Basso Ricci L, et al. In vivo tracking of T cells in humans unveils decade-long survival and activity of genetically modified T memory stem cells. *Sci Transl Med*. 2015;7(273): 273ra13.

34. Makar RS, Zhukov OS, Sahud MA, Kuter DJ. Thrombopoietin levels in patients with disorders of platelet production: diagnostic potential and utility in predicting response to TPO receptor agonists. *Am J Hematol*. 2013;88(12): 1041-1044.

35. Dong-Feng Z, Ting L, Yong Z, Cheng C, Xi Z, Pei-Yan K. The TPO/c-MPL pathway in the bone marrow may protect leukemia cells from chemotherapy in AML Patients. *Pathol Oncol Res*. 2014;20(2):309-317.